

# Core-Modified Expanded Porphyrins: New Generation Organic Materials

TAVAREKERE K. CHANDRASHEKAR\* AND SUNDARARAMAN VENKATRAMAN

Department of Chemistry, Indian Institute of Technology, Kanpur 208 016, India

Received February 3, 2003

## ABSTRACT

Even though the first expanded porphyrin was reported in the mid-1960s, the advances in its chemistry are more recent. New and powerful synthetic methods have facilitated the availability in affordable quantities of expanded porphyrins in general and core modified systems in particular. This has stimulated interest in studying various properties pertaining to their potential applications in biomedicine and materials chemistry. In this Account, we not only summarize the details of the synthetic methodologies reported, but we also highlight studies that focus on the structural diversity, aromaticity, and anion and cation binding abilities of expanded porphyrins.

## 1. Introduction

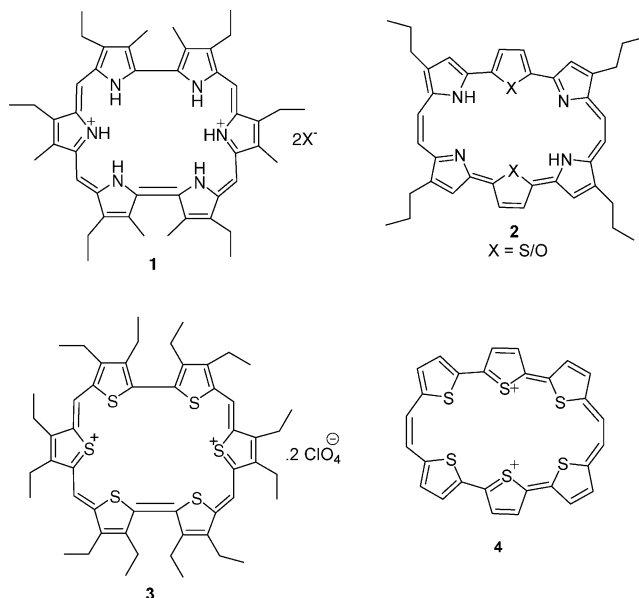
Expanded porphyrins are a class of conjugated macrocyclic compounds in which pyrrole rings are linked to each other in a cyclic fashion through *meso* carbon bridges. Unlike porphyrins, which are 18  $\pi$ -electron systems, the expanded porphyrins contain more than 18  $\pi$ -electrons in their conjugated pathway. The number of  $\pi$ -electrons can be increased either by increasing the conjugated double bonds between the four pyrrole rings or by increasing the number of pyrrole rings to five or more.<sup>1a</sup> The expanded porphyrins due to the increased number of donor atoms and varying cavity sizes are important for metal coordination, anion binding, and in favorable cases anion transport, as sensitizers for Photodynamic therapy (PDT), as contrasting agents in magnetic resonance imaging (MRI), and as radiation therapy enhancer, three rapidly developing biomedical applications,<sup>1b</sup> and also as non-linear optical materials<sup>1c</sup> and for studying fundamental issues related to aromaticity.

The electronic structure and the reactivity of expanded macrocycles can be controlled by altering the core of the

Tavarekere K. Chandrashekar was born in Shimoga, India, in 1956. He received his Masters from the University of Mysore in 1978. He earned his Ph.D. from the Indian Institute of Science, Bangalore, under the supervision of Prof. V. Krishnan in 1982. After Postdoctoral work with Prof. Hans VanWilligen (1982–84) at University of Massachusetts, Boston, and with the late Prof. G. T. Babcock (1984–86) at Michigan State, East Lansing, he joined the faculty at Indian Institute of Technology, Kanpur, where he is full professor since 1995. He spent a year (1993–94) on sabbatical with Prof. E. Vogel at University of Köln, Germany, as an Alexander van Humboldt Fellow.

Sundaraman Venkatraman was born in Thiruvavur, India, in 1977. He completed his Masters from Pondicherry University in 1999 and joined Indian Institute of Technology, Kanpur where he is pursuing his Ph.D. under the supervision of Prof. T. K. Chandrashekar.

Chart 1

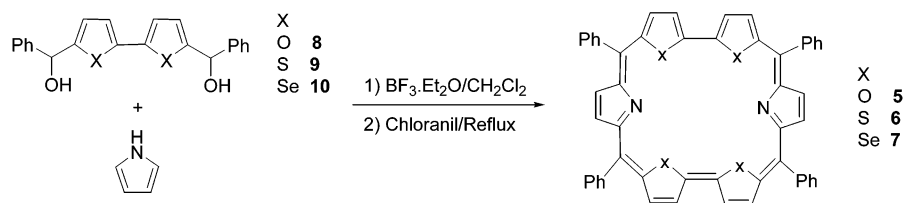


porphyrins<sup>1d</sup> involving substitution of one or more heteroatoms such as O, S, Se, or Te for pyrrole NH, leading to the formation of “core-modified expanded porphyrins”. Core-modified expanded porphyrins retain the basic framework of porphyrin macrocycle but have altered electronic, photochemical, optical properties while retaining aromatic character.

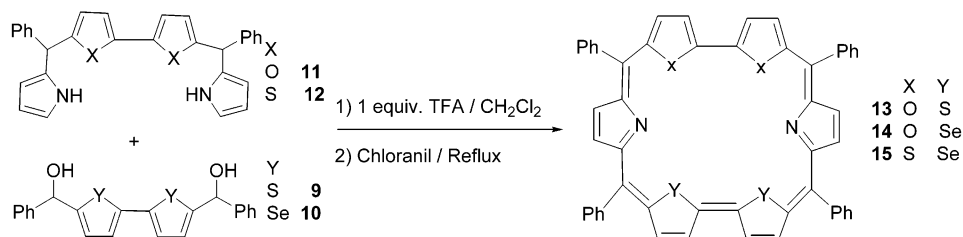
Recently, several groups have contributed significantly to the development of core-modified expanded porphyrin chemistry, with emphases on synthesis, structure, and reactivity. Acid-catalyzed condensation of appropriate precursors under mild conditions or oxidative coupling reactions where direct pyrrole–pyrrole links can be generated at the final step of the reaction have proven highly successful for the synthesis of a range of expanded porphyrins.<sup>1a,2</sup> From a structural perspective, expanded porphyrins with *meso* aryl substituents show a rich structural diversity where one or more heterocyclic rings exhibit an unusual 180° ring flipping leading to partially inverted structures,<sup>3</sup> including N-confused macrocycles.<sup>4</sup> It is shown that the structural preference, inverted versus planar, is very sensitive to the *meso* substituents. Reactivity studies have mostly concentrated on the ability of these species to bind anions and cations. Expanded porphyrins in their free base form have affinity for transition metal cations while in their protonated form they bind anions.<sup>5</sup> Anions are held by weak hydrogen bonding and electrostatic interactions. This Account aims to highlight the synthetic routes developed for the preparation of *meso* aryl expanded porphyrins, understand their structural diversities, analyze their aromatic behavior, and summarize their coordination ability regarding both anions and transition metal cations. Due to the limitations of space, we emphasize in this article only *meso* aryl 26  $\pi$

\* Corresponding author. E-mail: tkc@iitk.ac.in. Fax: +91-512-2597282/2597436/2590007.

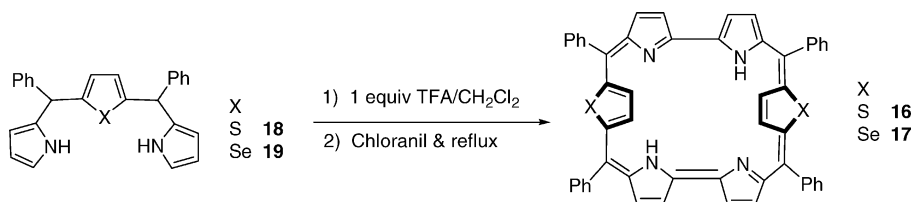
Scheme 1



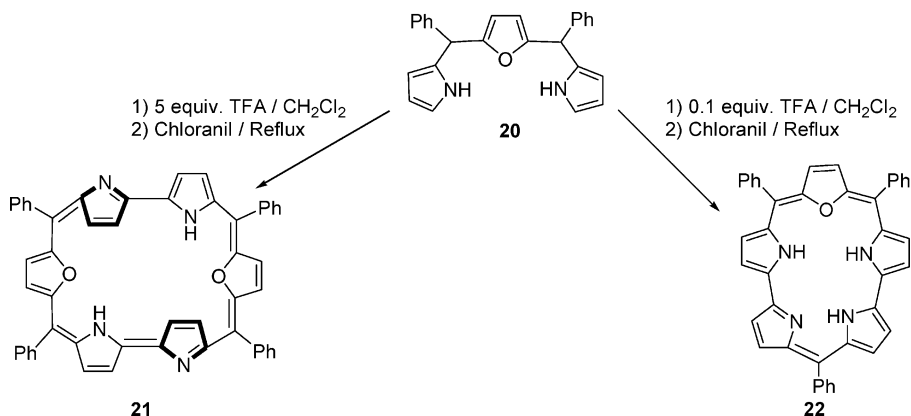
Scheme 2



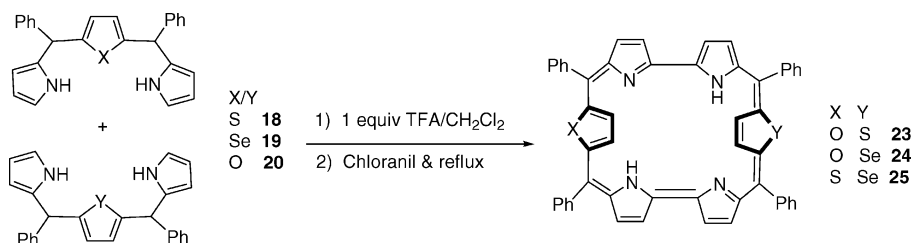
Scheme 3



Scheme 4



Scheme 5

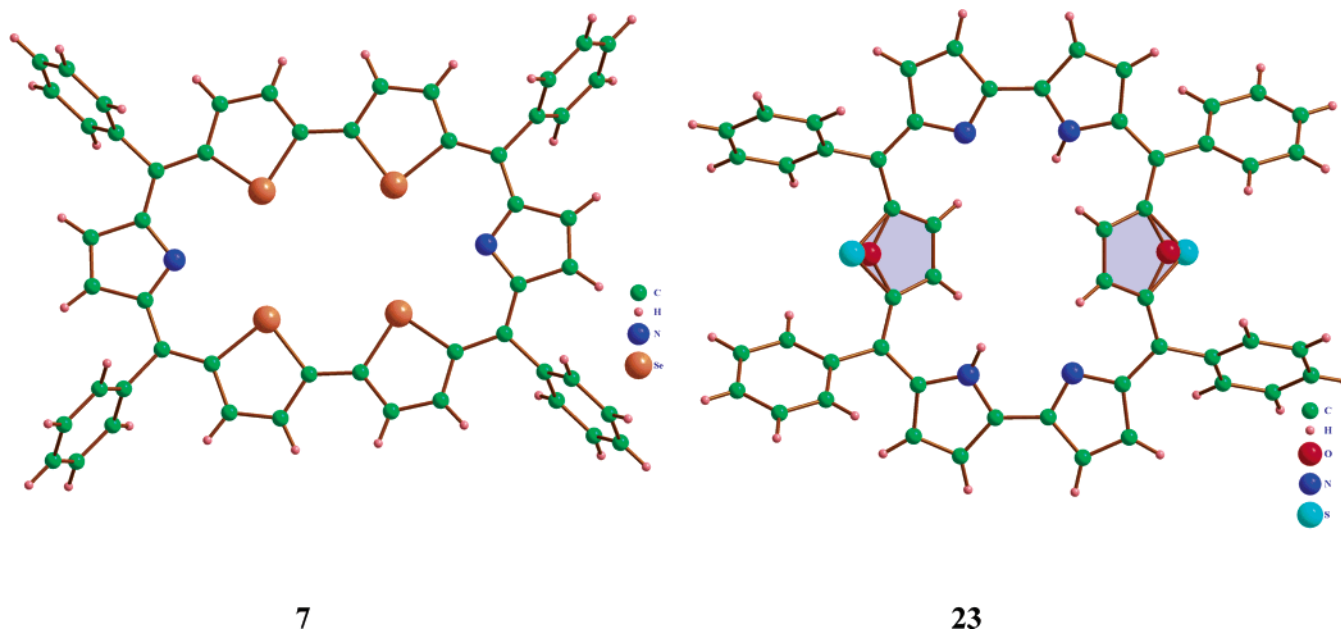
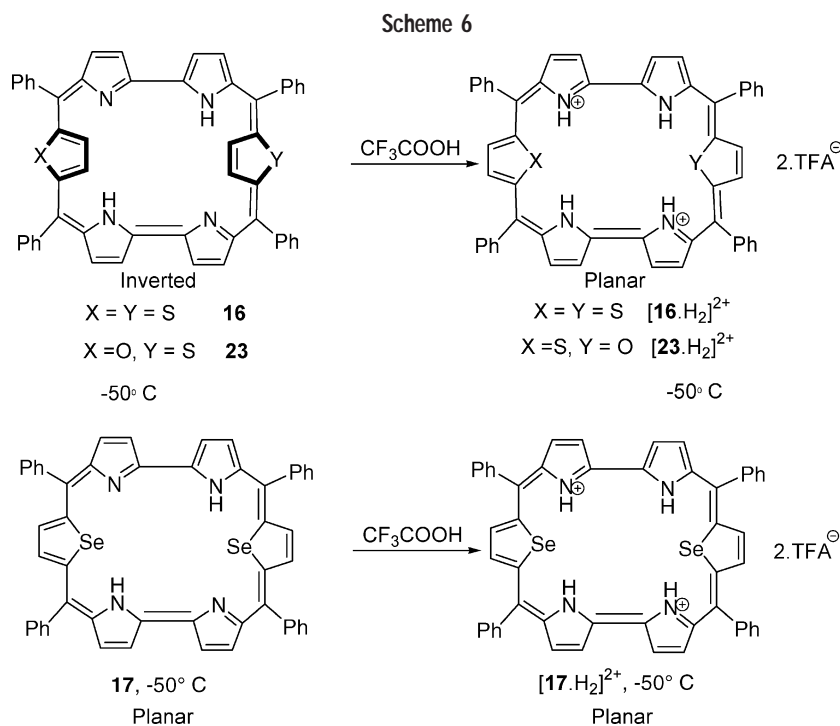


rubyrins,  $30 \pi$  heptaphyrins, and  $34 \pi$  octaphyrins. Further, material reviewed recently in the *Porphyrin Handbook*<sup>1a</sup> is excluded.

## 2. Rubyrins

Expanded porphyrins containing  $26 \pi$ -electrons can be constructed by either connecting six pyrrole/heterocyclic

rings with four *meso* carbons or four pyrrole/heterocyclic rings with eight conjugated double bonds between them. The first type with four *meso* carbons are referred as rubyrins because of their dark orange coloring in dichloromethane solution and the second type as tetravinylous porphyrins. In this section, the literature work on core-modified rubyrins will be highlighted.

FIGURE 1. X-ray structures of **7** and **23**.

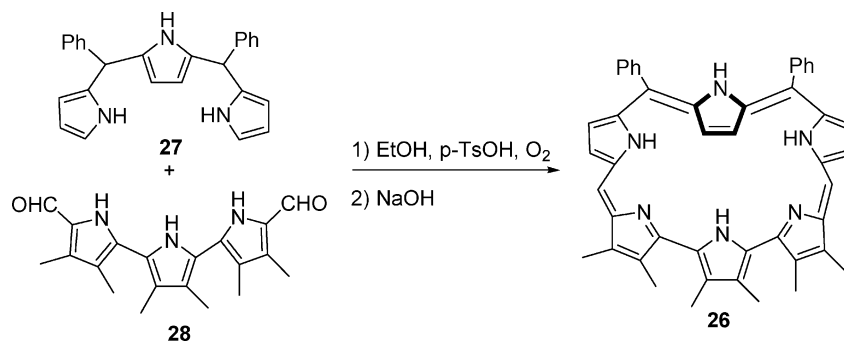
Sessler and co-workers<sup>6</sup> were the first to report the synthesis of hexapyrrolic 26  $\pi$  rubyrin **1**. Later on, efforts of Vogel,<sup>7</sup> Cava,<sup>8</sup> and Ibers<sup>9</sup> resulted in syntheses of hetero analogues **2**, **3**, and **4**. Either acid-catalyzed condensations of appropriate precursors or McMurry-type reductive couplings were made use of in these syntheses. Difficulties associated with syntheses of precursors, instability of precursors in some cases, and poor yields of final products in other instances provide a powerful incentive to develop easier and more efficient synthetic methods.

We reported the syntheses of *meso* aryl rubyrins,<sup>10</sup> containing heteroatoms in 1997. Specifically, tetraoxa **5**, tetrathia **6**, and tetraseleno **7** rubyrins were synthesized by acid-catalyzed condensation between bifuran/

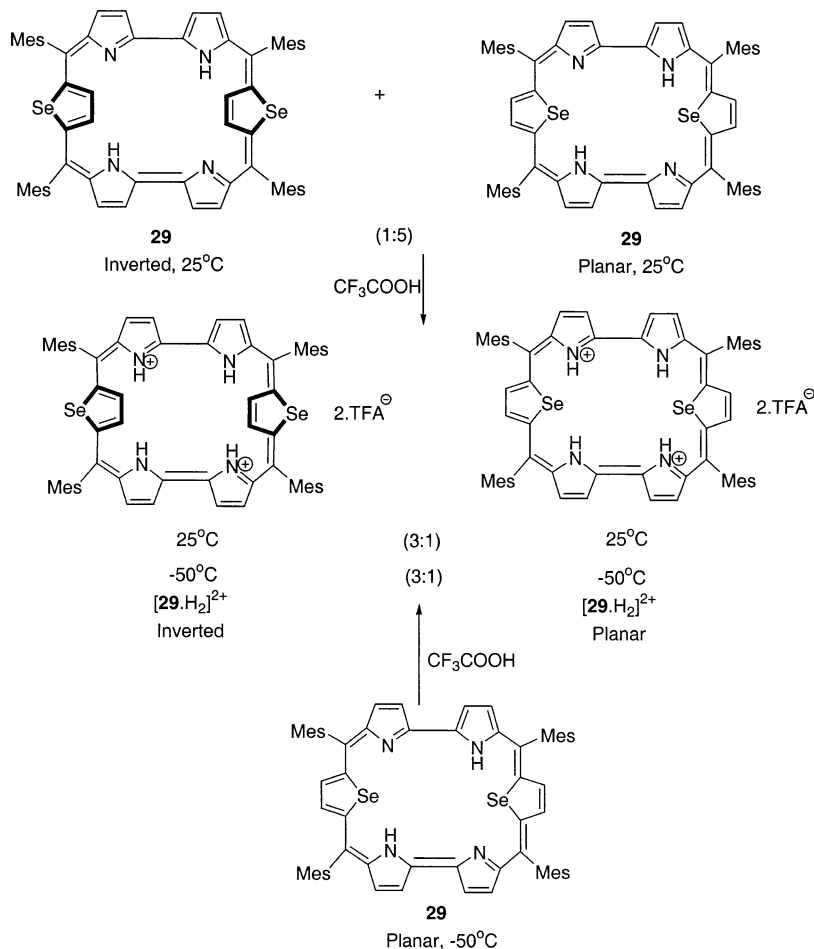
bithiophene/biselenophene diol **8/9/10** and pyrrole (Scheme 1). Later on, we used a [4+2] acid-catalyzed reaction<sup>11</sup> of heteroatom-containing tetrapyrromethanes **11** and **12** with **9** and **10** to synthesize rubyrins containing three different heteroatoms **13**, **14**, and **15** in 20–30% yields (Scheme 2). Detailed UV–vis and <sup>1</sup>H NMR spectroscopic studies on free base and the corresponding dication revealed their aromatic nature.<sup>10</sup> The cyclic voltammetric data not only confirmed the aromatic nature but also revealed (a) easier oxidation and reduction, (b) stabilization of both HOMO and LUMO, and (c) significant reduction in HOMO–LUMO gap relative to the *meso* aryl porphyrins.<sup>11</sup>

Recently, oxidative coupling methodologies have been

Scheme 7



Scheme 8



explored for the syntheses of expanded porphyrin systems.<sup>12</sup> Using this methodology, we<sup>13</sup> reported the synthesis of rubeans **16** and **17** by self-coupling of the modified tripyrranes **18** and **19** (Scheme 3). On the other hand, the self-coupling product of oxatripyrrane **20** depends on the amount of acid catalyst used.<sup>14</sup> At 5 equiv of trifluoroacetic acid (TFA), the expected 26  $\pi$ -electron oxarubyrin **21** was formed, while at 0.1 equiv of TFA, ring-contracted 22  $\pi$  oxasmaragdyrin<sup>15</sup> **22** was isolated. The oxidative coupling reactions of two different modified tripyrranes under dilute conditions were also attempted by our group.<sup>14</sup> Depending upon the tripyrranes used, **18** and **19** or **20**, different modified rubeans **23**, **24**, or **25** containing three

different heteroatoms were isolated (Scheme 5). UV-vis and <sup>1</sup>H NMR data confirmed their aromatic nature.

**2.1. Structure of meso Aryl Rubeans.** Unlike the  $\beta$ -pyrrole substituted rubeans **1**, **2**, and **3**, the meso aryl rubeans show rich structural diversity. Three different types of structures have been observed for meso aryl rubeans both in solution and in solid state.<sup>3</sup> They are planar as in **5**, **6**, or **7**, where all the four heteroatoms are pointing toward the ring current region and the  $\beta$ -CH protons projecting away. In the partially inverted structure, as in **16** and **23**, the two thiophene or one thiophene and one furan ring linked to the bipyrrolic units have undergone a 180° ring flipping in such a way that the  $\beta$ -CH

Scheme 9

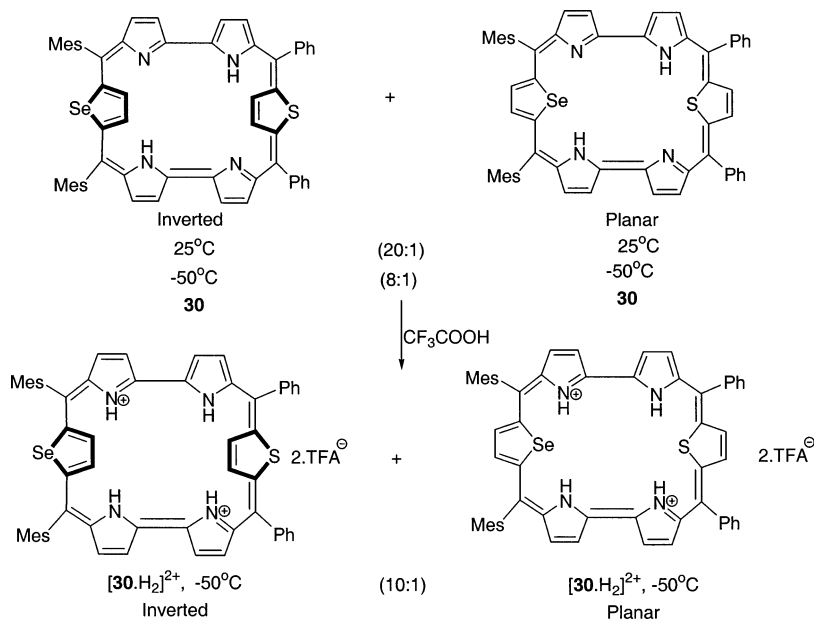


Table 1

compound	binding constant $K/M^{-1a}$		
	KF	NaN <sub>3</sub>	K <sub>2</sub> CO <sub>3</sub>
<b>6</b>	49	767	1290
<b>7</b>	29	130	224
<b>13</b>	78	896	1372
<b>14</b>	42	374	674

<sup>a</sup> The estimated error is  $\pm 5\%$ .

protons of thiophene/furan point toward the ring current region and the sulfur/oxygen atoms point away from the ring current region<sup>14</sup> (Figure 1). On the other hand, **21** also shows a partially inverted structure where one of the pyrrole ring on each bipyrrolic unit exhibits a 180° ring flipping, giving rise to a new type of inverted structure.<sup>3</sup>

The solution studies also reveal the existence of structural diversity. It was possible to identify easily the planar or the inverted structures by the difference in the chemical shifts of  $\beta$ -CH protons.<sup>14</sup> These protons resonate in the aromatic region (9–11 ppm) for the planar form, while for the inverted form they resonate in the -1 to -6 ppm region, owing to the aromatic ring current. For example, the <sup>1</sup>H NMR spectrum of **21** in the protonated form exhibits a “doublet of doublet” in the region -1.8 to -2 ppm assigned to the inverted  $\beta$ -CH protons of the bipyrrolic unit, while the NH protons of the inverted pyrrole ring resonates as a singlet at 16 ppm. The dynamics of converting an inverted structure to a planar structure and vice versa was also studied. For example, the rubeirins **16** and **23** show inverted structure in their free base form, while upon protonation they revert to the planar form. On the other hand, rubeirin **17**, exhibits only a planar structure both in its free base and protonated form (Scheme 6). To further understand the structural behavior of *meso* aryl rubeirins, Sessler and co-workers<sup>16</sup> reported the synthesis of a new all-aza isomer of rubeirin **26** by acid-catalyzed condensation of 1:1 mixture of diphenyltripyrane **27** and diformylhexamethylterpyrrole **28** (Scheme 7).

The X-ray structure of protonated **26** reveals a 180° flipping only in the central pyrrole ring of the diphenyltripyrane unit, in accordance with the structure expected for *meso* aryl rubeirins.

**2.2. Effect of *meso* Substituents on the Structure of Rubeirins.** Increase in the steric bulk of the *meso* substituents is found to have an effect on the structure of *meso* aryl rubeirins. For example, changing the *meso* substituents from *meso* phenyl to *meso* mesityl in the precursor tripyrranes upon oxidative coupling yielded both planar and inverted rubeirins.<sup>17</sup> The ratio of the planar and inverted forms were found to be dependent on the temperature and the state of protonation. For example, the results of <sup>1</sup>H NMR studies of *meso* mesityl rubeirin **29**, synthesized from the oxidative coupling reaction of *meso* mesityl tripyrrane, are summarized in Scheme 8. Oxidative coupling reaction of *meso* mesityl containing selenatripyrrane and *meso* phenyl thiatripyrrane gave rubeirin **30** containing *meso* mesityl groups on one side and *meso* phenyl groups on the other. Compound **30** also exists in both planar and inverted forms, as shown in Scheme 9.

It is apparent from the above discussion that the *meso* aryl rubeirins exhibit dynamic structural behavior, and that structure is quite sensitive to the *meso* substituents present, nature of the heteroatom, the state of protonation and the temperature. In favorable cases, it is possible to convert one to the other by simple chemical modification.

**2.3. Metal Complexes of Rubeirins.** We have recently investigated the ligational behavior of *meso* aryl core-modified rubeirins<sup>18</sup> toward Rh(I). Rubeirins form both monometallic and bimetallic complexes. Two types of bimetallic complexes have been isolated (Scheme 10). In the first type, both rhodium atoms are projected above the mean plane of the rubeirin (plane defined by four *meso* carbons), while in the second, one rhodium atom is projected above and the other is found below the mean plane. The single-crystal X-ray analysis of one of the

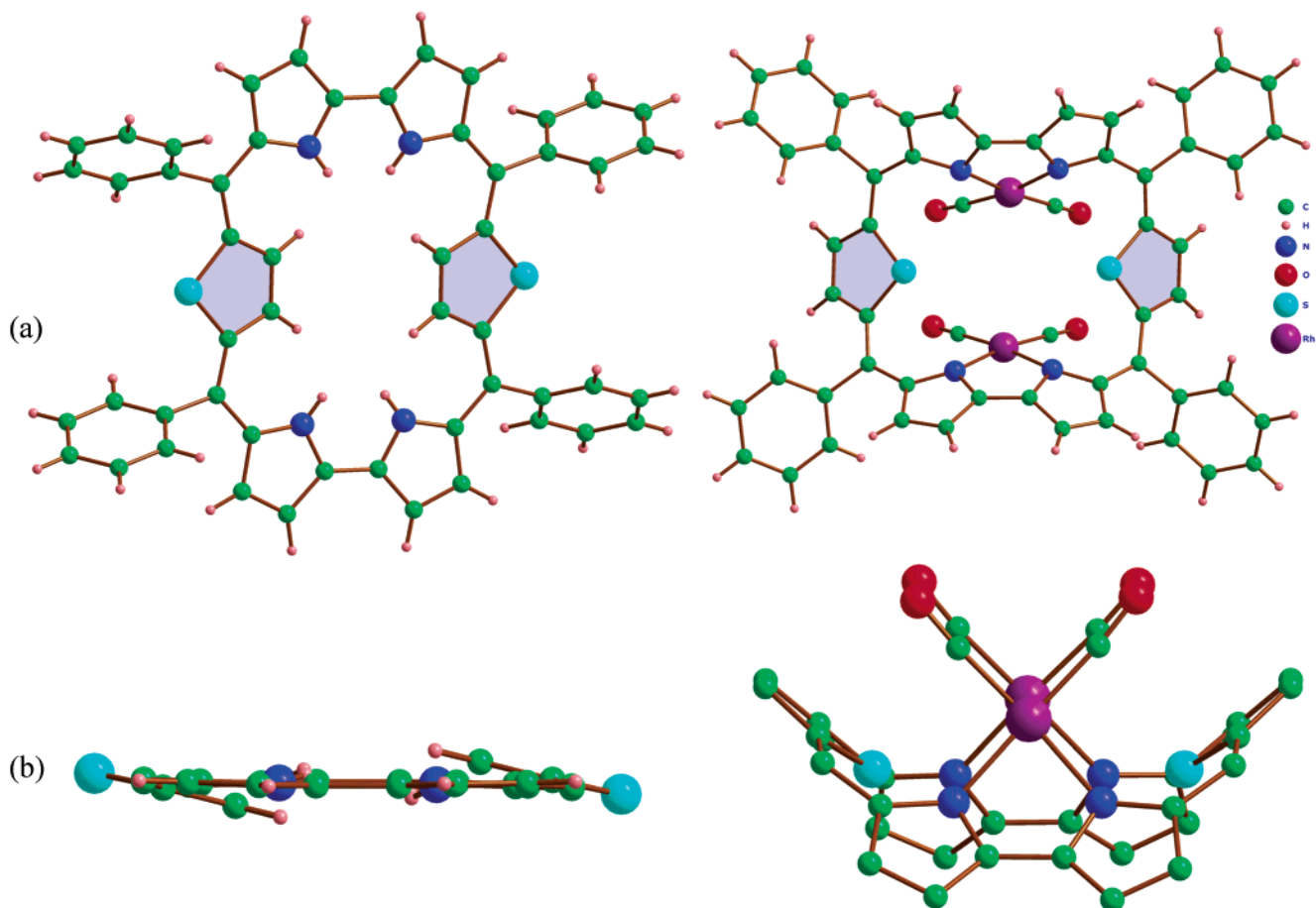
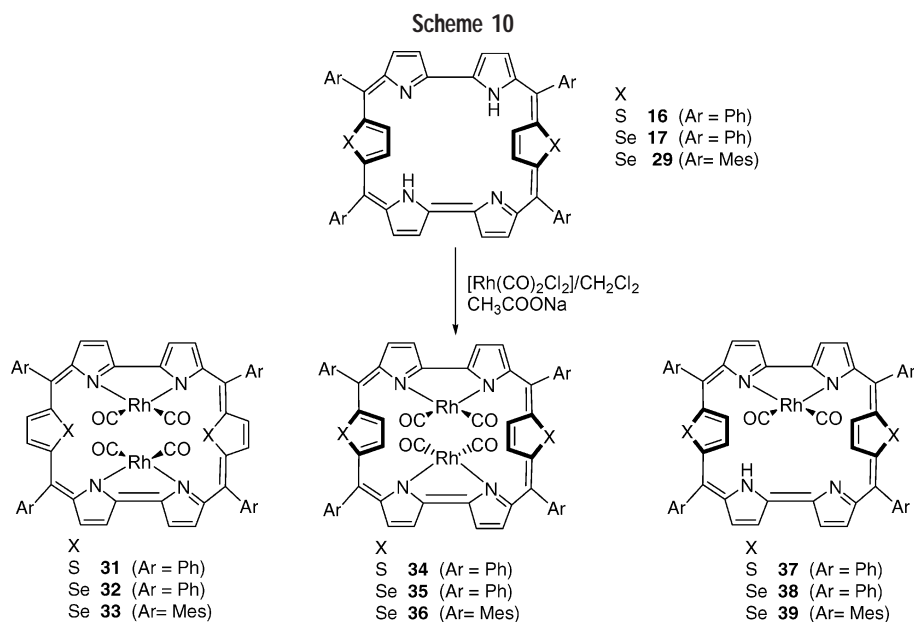


**FIGURE 2.** A comparison of X-ray structures of **16** and its dirhodium complex **31** (a) top view (b) side view. The ring flipping upon metal binding is highlighted.

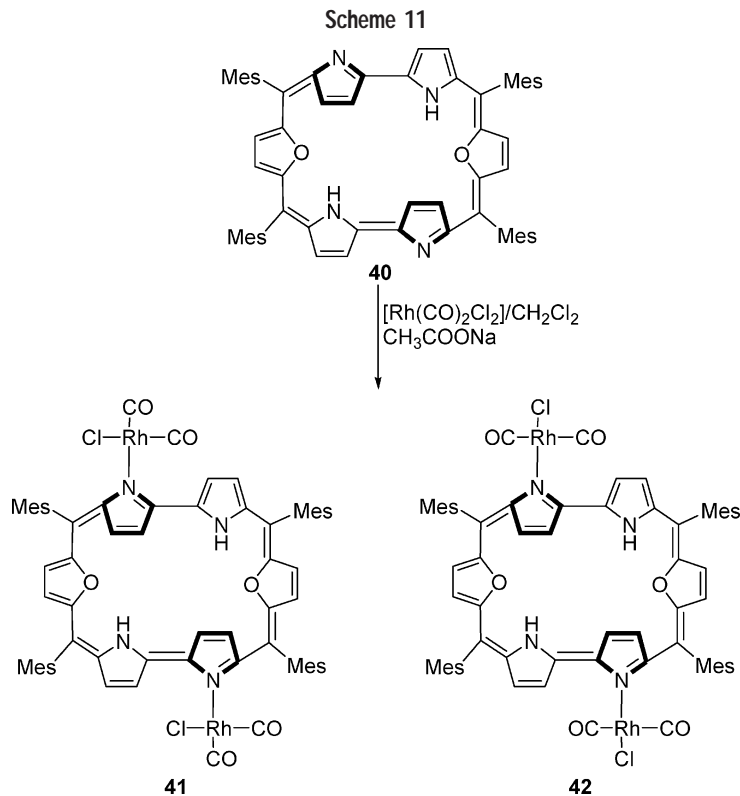


bimetallic complexes shows bowl-shaped symmetric structure, where both rhodium atoms project above the mean plane at an angle of  $71.73^\circ$ .

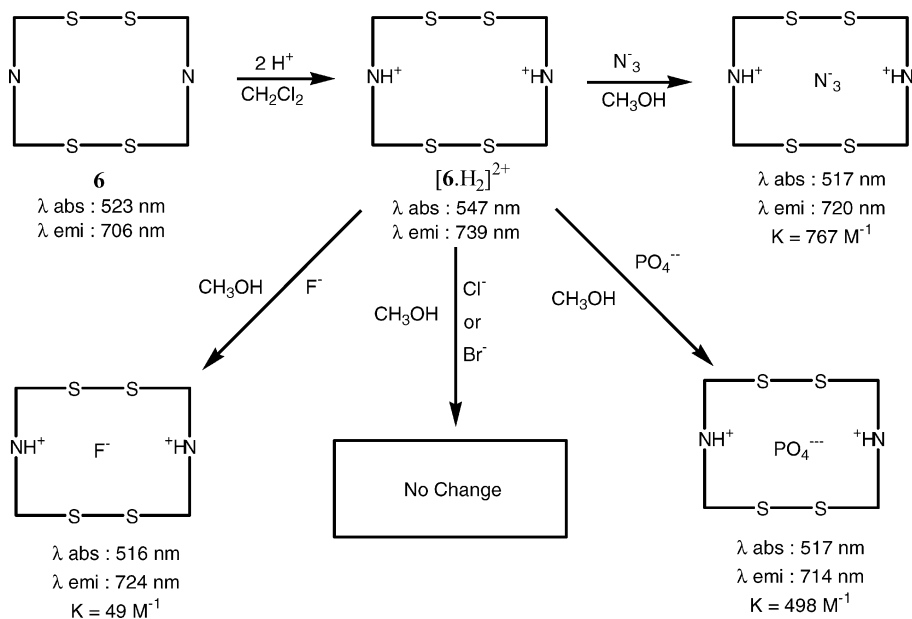
Another interesting observation in the metal complexes is metal-induced ring flipping upon coordination. This metal-induced ring flipping was dependent on the nature of

the coordination and the number of metals coordinated. For example, in the mono metallic complexes **37–39**, the original structure of the free base was retained upon Rh coordination, while for the bimetallic complexes **31–33**, the X-ray structure reveals  $180^\circ$  ring flipping (Figure 2) for the complex, where both the metal atoms are projected

Scheme 11



Scheme 12



above the mean plane probably due to the ring strain. On the other hand, in the bimetallic complex, where the rhodium atom is located above and below the mean plane of the rubyrin **34–36**, no ring flipping was observed.

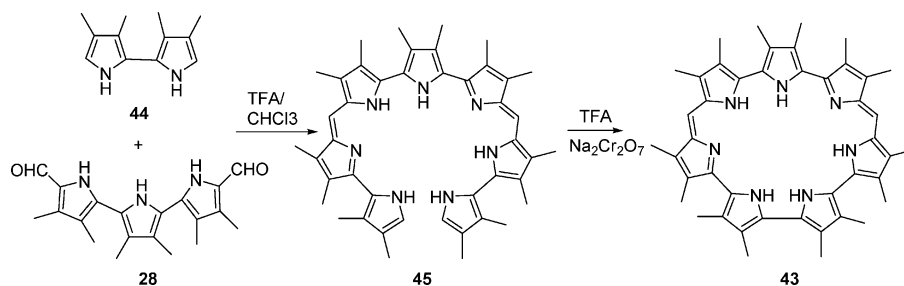
The dioxarubyrin **40** exhibits a different mode of binding. In this case, the Rh is bound to the inverted pyrrole ring nitrogen only at the periphery as in **41** and **42**, leaving the central cavity of the rubyrin empty (Scheme 11).<sup>18</sup>

**2.4. Anion Binding Studies.** Protonation of two pyrrole nitrogens leads to the formation of dicationic species with two positive charges delocalized inside the cavity. Thus, the diprotonated form of rubyrins are expected to have

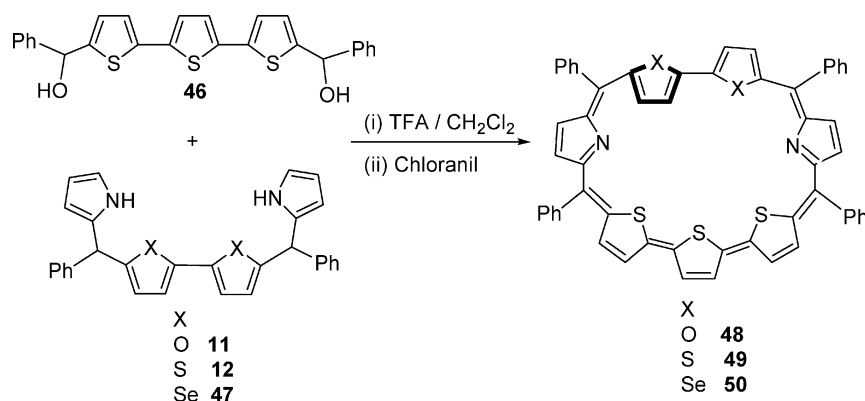
affinity for the anions. For example, spectral titrations of a methanolic solution of diprotonated  $[6.H_2]^{2+}$  with anions result in decrease in absorbance, a blue shift of the Soret band by about 30 nm, and a blue shift of the emission band by about 15 nm together with enhanced emission intensity. These observations suggest anion binding,<sup>5</sup> and the binding constants evaluated by an analysis of absorption data vary as  $N_3^- > AMP > F^-$  (Scheme 12).<sup>10</sup>

A comparison of binding constants for the binding of  $F^-$ ,  $N_3^-$ , and  $CO_3^{2-}$  for rubyrins **6**, **7**, **13**, and **14** are made in Table 1. It is shown that the binding constants depend on (a) the complementarity of the anion size and the cav-

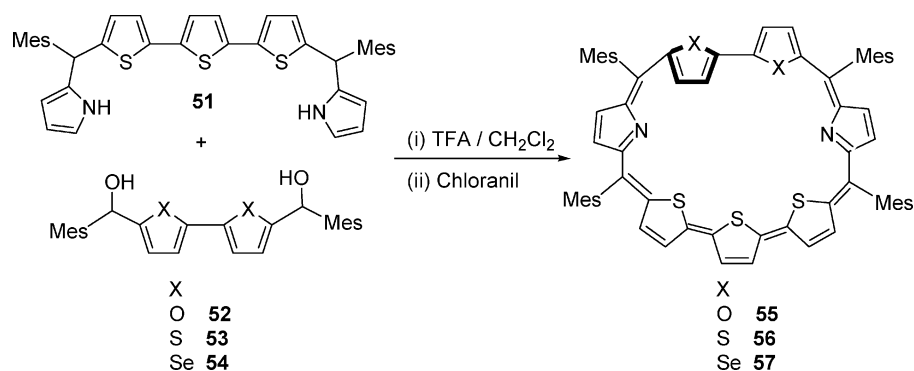
Scheme 13



Scheme 14



Scheme 15



ity size available and (b) the number of hydrogen bonding sites available inside the cavity. The lower binding constants observed for F<sup>-</sup> complexes reflect mismatch of the sizes of the F<sup>-</sup> ion and the rubein cavity.<sup>19</sup> In the core-modified rubeins, the cavity size will be different for rubeins, depending on the size of the heteroatoms. The binding constants observed for N<sub>3</sub><sup>-</sup> and CO<sub>3</sub><sup>2-</sup> complexes are orders of magnitude lower compared to the all-aza rubein complexes because of the decrease in the number of hydrogen bonding sites in **13**, **6**, **14**, and **7**. The higher value for the CO<sub>3</sub><sup>2-</sup> relative to the N<sub>3</sub><sup>-</sup> is in part attributed to the complete charge neutralization for CO<sub>3</sub><sup>2-</sup> as against partial charge neutralization for N<sub>3</sub><sup>-</sup> complex.

There is only one report on the solid-state structure of an anion complex of rubein. Specifically, Sessler and co-workers<sup>16</sup> reported the dichloro complex of **26**. There are two chloride ions, one above and one below the mean rubein plane and the anions are held by N–H···Cl hydrogen bonding interactions. In addition to the two

bound Cl<sup>-</sup> ions, there is one molecule of water incorporated in the structure.

### 3. Heptaphyrins

Heptaphyrins are expanded porphyrins in which seven pyrrole/heterocyclic rings are connected through *meso* carbon bridges. Sessler and co-workers<sup>20</sup> were the first to report synthesis of heptaphyrin **43** by acid-catalyzed condensation of diformyl hexamethylterpyrrole **28** with 2.5 equiv of tetramethylbipyrrole **44**, which afford the linear oligopyrrole **45** which upon subsequent oxidative ring closure in the presence of Na<sub>2</sub>Cr<sub>2</sub>O<sub>7</sub> in TFA afford **43** with two *meso* carbon bridges (Scheme 13). Despite fairly planar structure, **43** turned out to be nonaromatic.

We reported synthesis of a range of modified *meso* aryl 30 π-electron heptaphyrins<sup>21</sup> **48**–**50** and **55**–**57** through [4+3] and [5+2] acid-catalyzed condensation reactions of appropriate precursors (Schemes 14 and 15). Furthermore, we also exploited oxidative coupling reactions for the



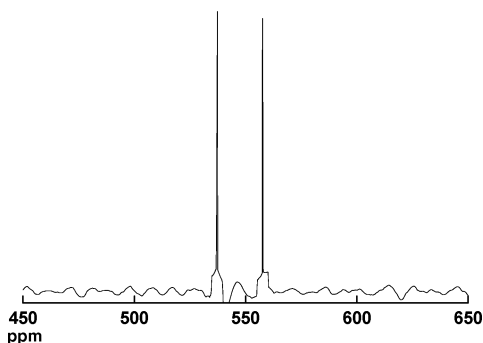


FIGURE 3. The  $^{77}\text{Se}$  NMR of **50** in  $\text{CDCl}_3$ .

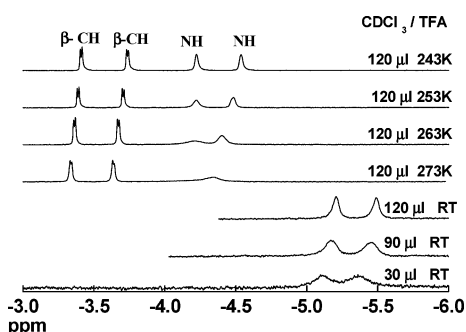


FIGURE 4. Temperature-dependent chemical shifts in the shielded region upon protonation for the inverted ring and NH protons of **50**. The diprotonated species was generated by adding TFA 10% (v/v) in  $\text{CDCl}_3$ .

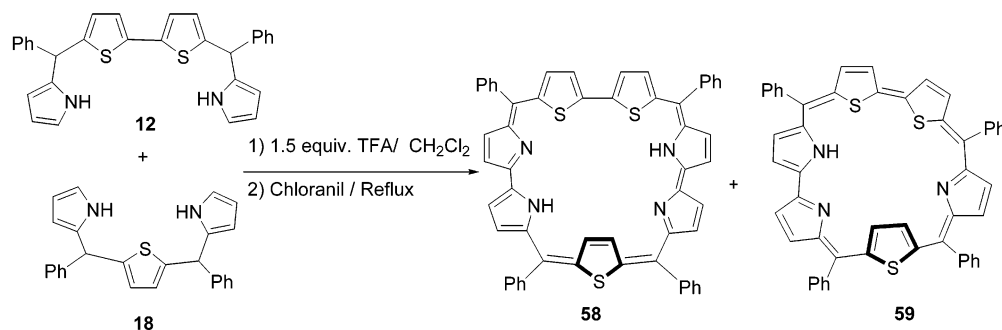
synthesis of heptaphyrins<sup>22</sup> (Scheme 16). In this reaction, in addition to the expected heptaphyrin **58**, a new isomer of rubyrin **59** was also isolated as byproduct.<sup>2c</sup>

Substitution of bulkier mesityl group for phenyl groups in the precursors **12** and **18** had a marked effect on the product distribution.<sup>22</sup> A [4+3] oxidative coupling of

mesityl derivatives **60** and **61** yielded a new heptaphyrin isomer **63** along with expected heptaphyrin **62** (Scheme 17).

**3.1. Structure of Heptaphyrins.** Like *meso* aryl rubyrins, *meso* aryl heptaphyrins also exhibit structural diversity. All the *meso* aryl core-modified heptaphyrins reported to date exhibit partially inverted structures in which one or more heterocyclic rings have undergone  $180^\circ$  ring flipping. The site of ring inversion and the number of inverted rings depend on the nature of the connectivity and the nature of the heteroatom. For example, in **64**, only two thiophene rings bearing Sulfur are inverted. Even though no single-crystal solid structure is reported for any of these heptaphyrins, detailed variable-temperature  $^1\text{H}$  NMR and 2-D NMR studies in addition to theoretical calculations unequivocally support the proposed structures.<sup>22</sup> For example, for **56**, (Chart 2) the  $^1\text{H}$  NMR spectrum shows a well-resolved “doublet of doublet” in the region  $-0.5$  to  $-2$  ppm, assigned to one of the inverted heterocyclic rings. Upon protonation, these resonances experience further shielding ( $-5$  to  $-5.2$  ppm), and the pyrrole NH proton resonates in the region  $-6.5$  to  $-7$  ppm, suggesting that the ring inversion is retained upon protonation. Further support for the proposed ring inversion in the bithiophene-like unit is drawn from the  $^{77}\text{Se}$  NMR spectrum of heptaphyrin **50**. Specifically, the  $^{77}\text{Se}$  NMR spectrum of **50** (Figure 3) shows two different signals at 557 and 537 ppm with respect to dimethyl selenide. This indicates that the two selenium atoms are in different environments, a finding that is best explained by assuming that one of the rings from the biselenophene unit has been inverted. The protonated spectra in the shielded region (Figure 4) clearly reveal that the ring inversion is retained upon protonation,

Scheme 16



Scheme 17

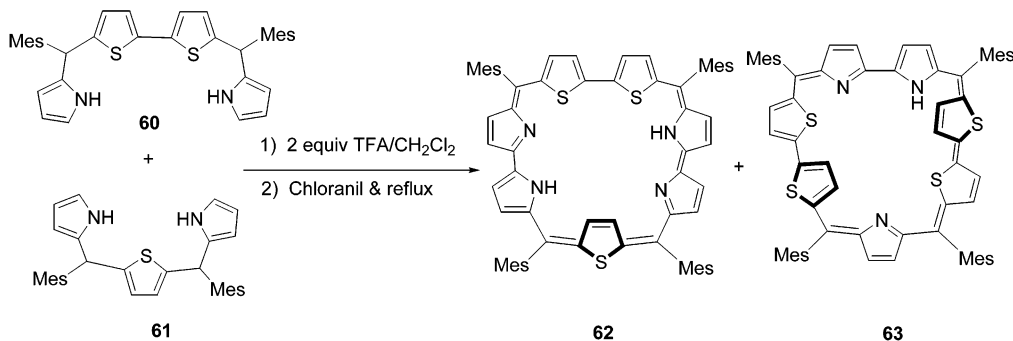
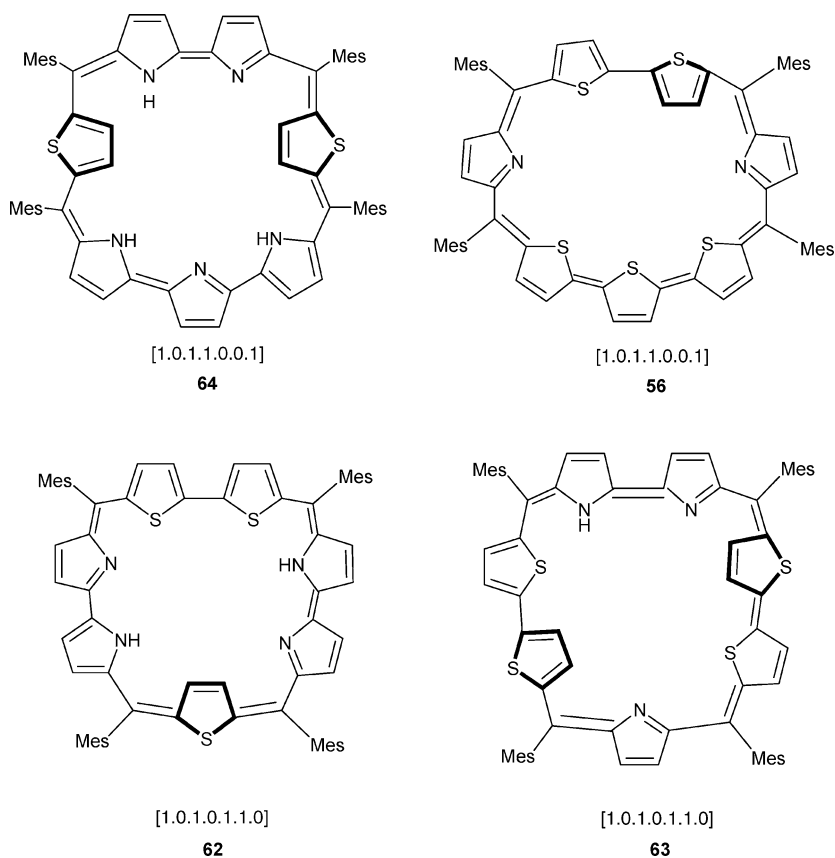
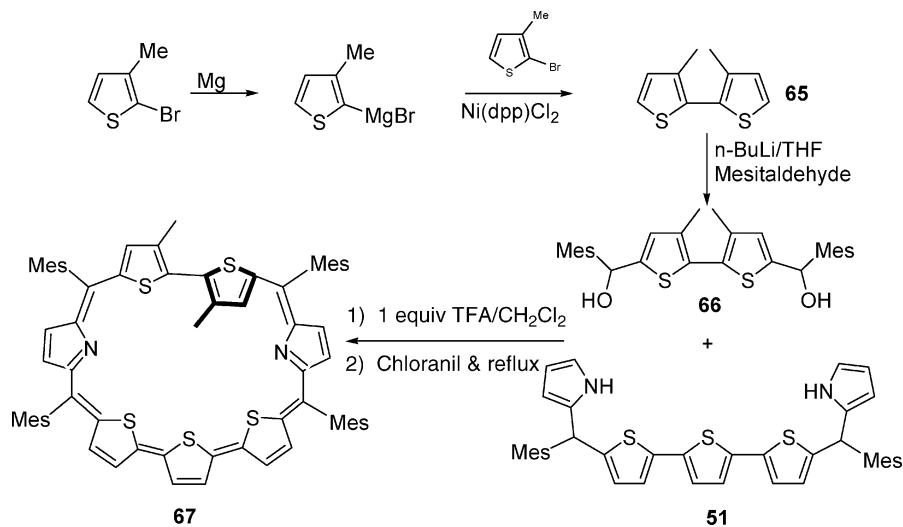


Chart 2



Scheme 18

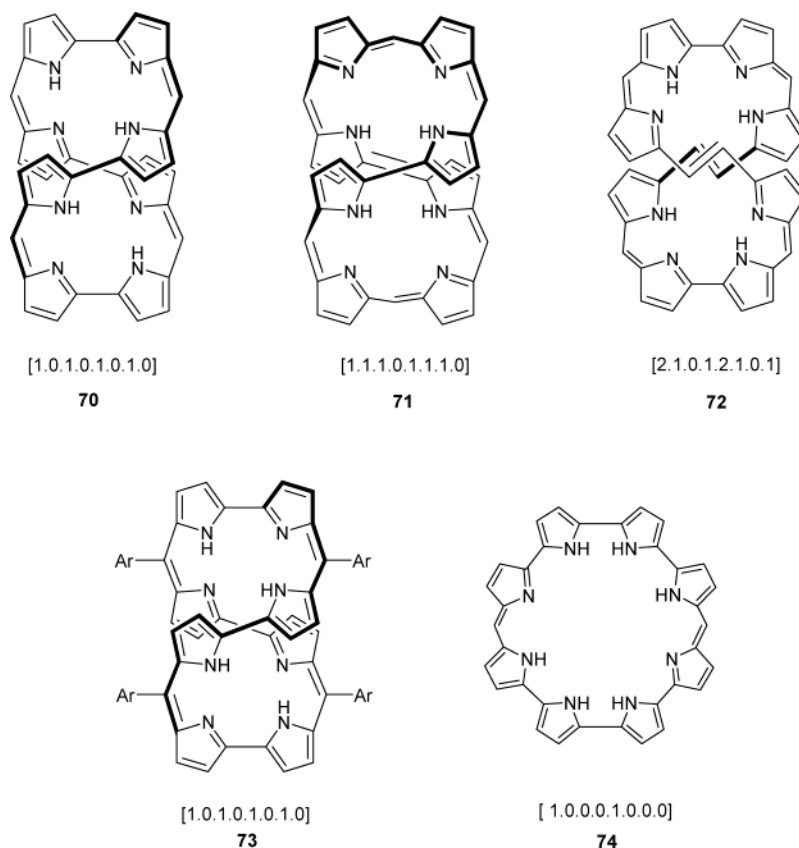


and as observed earlier, the ring inverted  $\beta$ -CH protons experience shielding upon protonation. Further confirmation for the proposed ring inversion in the bithiophene unit is available by studying an analogue of **50** bearing methyl groups on the  $\beta$  positions of the bithiophene unit. The requisite  $\beta$ -substituted bithiophene **65** precursor was synthesized from 3-methyl-2-bromothiophene. Reacting this latter starting material **65** with *n*-butyllithium and mesitaldehyde gave the diol **66** in 50% yield. Heptaphyrin **67** was obtained by a reaction of **66** with modified pentapyrrane **51** in 15% yield (Scheme 18).<sup>22</sup> The <sup>1</sup>H NMR spectrum of **67** resolved the doubts concerning the ring

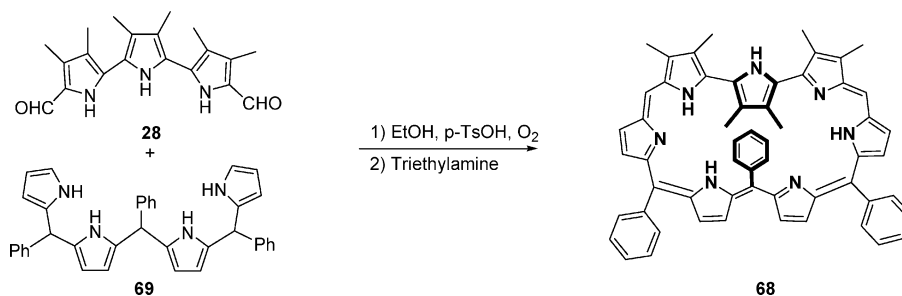
inversion in the macrocycle. In the ring-inverted state, of the two  $\beta$ -methyl groups, one experiences diatropic ring current and the other does not. Therefore, one would expect that the methyl groups should have different chemical shifts, one in the shielded region and the other in the normal region. In **67**, the two methyl groups resonate at  $-3.86$  and  $2.7$  ppm, thus confirming one ring inversion of the bithiophene unit and not in the trithiophene unit.

Very recently Sessler and co-workers<sup>23</sup> reported the synthesis of 30  $\pi$ -electron aromatic heptaphyrin **68** by a [4+3] condensation reaction (Scheme 19). This heptaphyrin **68**

Chart 3



Scheme 19



is unique in its structure. In solid state, **68** displays a figure-eight structure with one pyrrole ring inverted and one phenyl group “pointing inward” toward the center of the macrocyclic ring. However, in solution, **68** shows a flat structure with properties expected for aromatic 30  $\pi$  macrocycle.

**3.2. Spectroscopic Studies.** UV–vis spectral studies on heptaphyrins reveal the presence of intense Soret type of bands in the region 540–580 nm and Q-type bands in the region 650–1050 nm. The presence of greater number of heteroatoms and the effect of extended delocalization relative to rubryns are reflected in the red shift of the absorption bands. The  $\epsilon$  values for the Soret bands were on the order of  $10^5$ , those for the Q-bands were on the order of  $10^4$ , and these values are an order of magnitude higher than the nonaromatic heptaphyrin **43**. Furthermore, upon diprotonation (Figure 5) the absorption bands experience a further red shift (by 30–45 nm), which is typical of *meso* aryl expanded porphyrins, and the  $\epsilon$  values for

the protonated derivatives are slightly higher relative to the free base. The aromaticity of these heptaphyrins can be gauged by two parameters: (a) the energy of the Soret maximum, which is expected to go down as the number of  $\pi$  electrons are increased in the delocalization pathway; (b) the HOMO–LUMO gap, which is also expected to be reduced linearly with increase in  $\pi$  electrons in conjugation. Such a variation for both the parameters shown in Figure 6 follows linear correlation supporting the aromatic nature of the modified *meso* aryl heptaphyrins. Further support for the aromatic nature also comes from the observed  $\Delta\delta$  (difference in the chemical shifts of the most shielded and the most deshielded proton) values, which vary in the range 10.07–20.59 ppm for the heptaphyrins.<sup>22</sup>

## 4. Octaphyrins

Octaphyrins are macrocycles having eight pyrrolic/heterocyclic rings that are interconnected by *meso* carbons

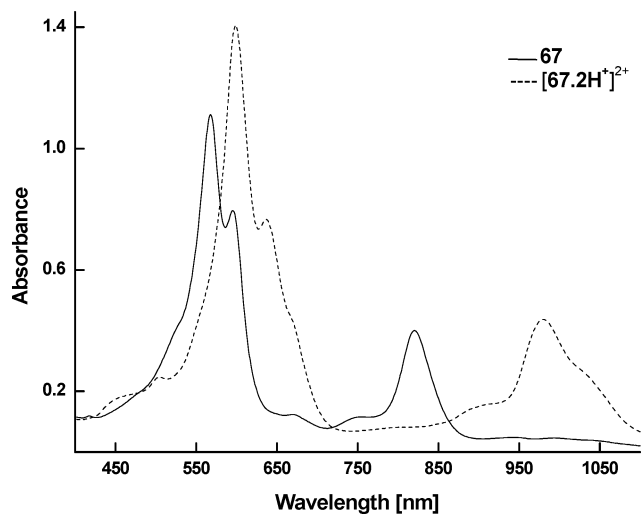
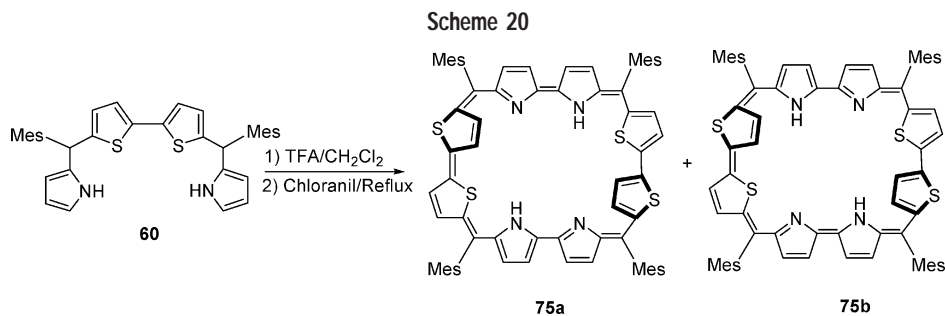


FIGURE 5. A comparison of absorption spectra of **67** (—) and  $[67.2\text{H}]^{2+}$  (---) in  $\text{CH}_2\text{Cl}_2$ .

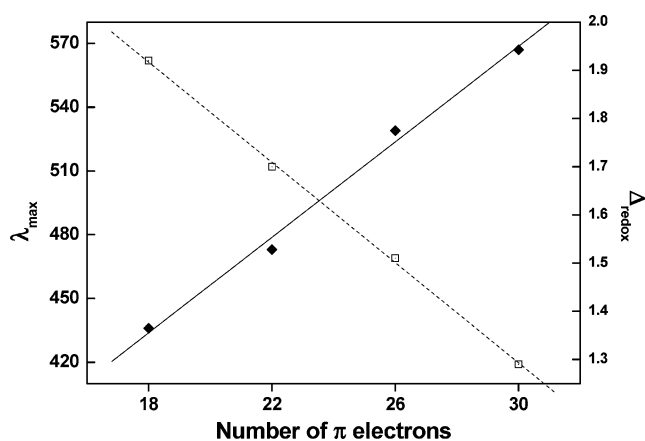


FIGURE 6. Variation of energy of Soret band ( $\blacklozenge$ ) and HOMO–LUMO gap ( $\square$ ) with increasing number of  $\pi$  electrons.

in cyclic fashion. Vogel and co-workers<sup>24</sup> were the first to report the formation of cyclooctapyrroles during the synthesis of porphyrin isomers. Later, persistent efforts from the same group<sup>25</sup> resulted in a variety of octaphyrins **70**, **71**, and **72**. Setsune and co-workers<sup>26</sup> reported the synthesis of octaphyrin **73** containing *meso* aryl substituents. Structural studies on these systems reveal the existence of figure eight conformations in solid state, thus leading to a loss in aromatic character. The octaphyrins **70** and **73**, despite having  $(4n + 2)$   $\pi$ -electrons, turned out to be nonaromatic. To avoid figure-eight conformation, Sessler and co-workers<sup>20</sup> reduced the number of bridging carbons and synthesized **74** by oxidative coupling

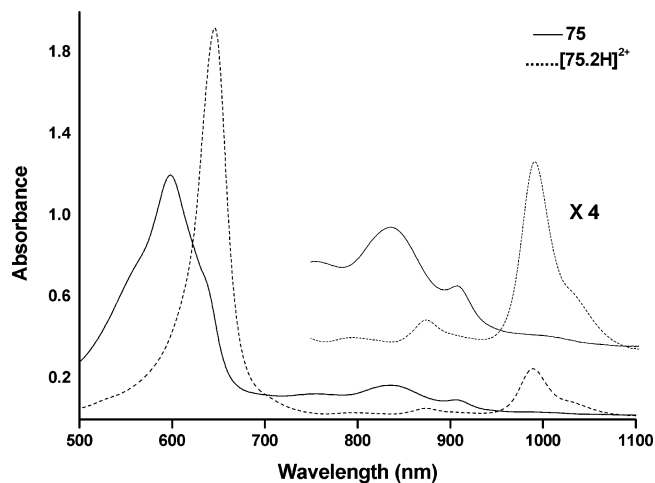
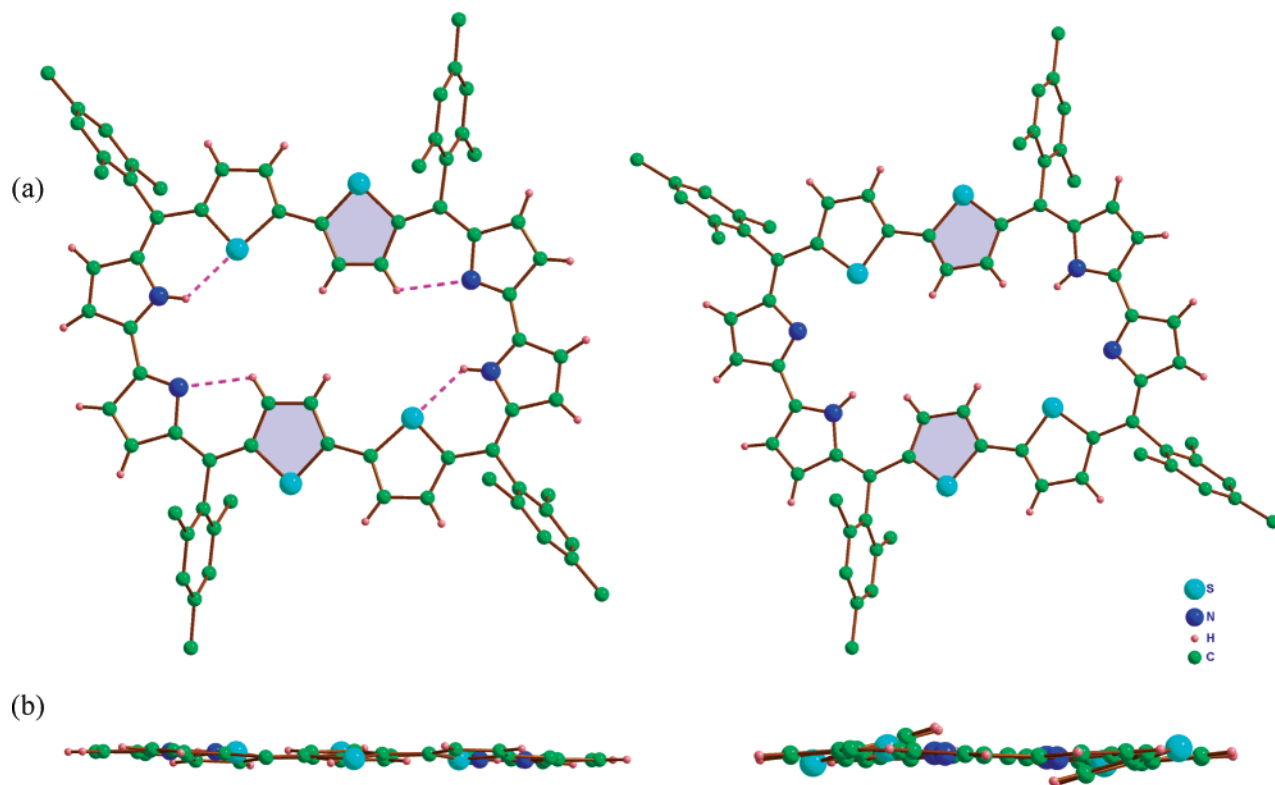


FIGURE 7. A comparison of absorption spectra of **75** (—) and  $[75.2\text{H}]^{2+}$  (---) in  $\text{CH}_2\text{Cl}_2$ .

of tetrapyrrole with bipyrrole precursors. Despite its nontwisted structure, **74** did not exhibit aromatic features. More recently, Osuka and Furuta<sup>27</sup> were successful in isolating *meso* aryl 36  $\pi$ -electron octaphyrin, which was also found to display a figure eight conformation. An analysis of the syntheses described above reveals that the polycyclic pyrroles undergo a twisting around *meso* bridges, which is responsible for the loss of planarity and hence the aromaticity. Therefore, arresting the twist in the molecule is a key step in sustaining the required planar form. One way to minimize such a twisting is to replace a few pyrrole nitrogens by heavier heteroatoms and to increase the steric bulk at the *meso* carbons, thereby making *meso* substituents more orthogonal to porphyrin plane. This idea drawn from the retro synthetic analysis encouraged us to attempt an acid-catalyzed oxidative self-coupling of tetrapyrane<sup>28</sup> **60**. This reaction on workup gave a lustrous bronze solid. It was identified as a 34  $\pi$ -electron modified octaphyrin **75** (Scheme 20). The UV–vis spectrum of **75** in dry methylene chloride exhibits an intense Soret-type band [598 nm,  $(4.95, \log \epsilon)$ ] and a series of Q-bands [754 (3.95), 835 (4.1) and 906 nm (3.85)], and on diprotonation these bands experience red shift with increase in the  $\epsilon$  values (Figure 7).

Detailed  $^1\text{H}$  and 2-D NMR studies performed in two different solvents ( $d_8$ -toluene and  $\text{CDCl}_3$ ), between the temperature range 330–208 K of **75**, provided evidence consistent with the presence of two tautomers (**75a** and **75b**) in solution, and separate sets of peaks observed for both. Furthermore, in both the tautomers, one thiophene ring of each bithiophene unit is inverted, as inferred from



**FIGURE 8.** A comparison of X-ray structures of **75a** and **75b** (a) top view (b) side view. The dotted lines show hydrogen bonding interactions. The inverted rings have been shaded.

the observation of  $\beta$ -CH protons of these rings in the shielded region. For example, for **75a**, in toluene- $d_8$  at 248 K, two sharp doublets appear at  $-5.3$  and  $-5.89$  ppm that are assigned to  $\beta$ -CH protons of the inverted thiophene rings. On the other hand, **75b** showed a less planar structure relative to that of **75a**, as inferred by the greater number of peaks observed. In this case, four doublets are observed in the region  $-3.28$  to  $-3.61$  ppm in toluene- $d_8$  assigned to the  $\beta$ -CH protons of the inverted thiophene rings. The two pyrrole NH protons now resonate as two broad singlets at  $-0.8$  and  $-4.16$  ppm, a finding consistent with their magnetic inequivalence. An estimate of  $\Delta\delta$  values for **75a** is 17.32 ppm and for **75b** is 14.89 ppm in toluene- $d_8$ . Thus, the  $^1\text{H}$  NMR data in conjunction with the UV-visible data give a strong evidence for the aromatic nature of **75**.

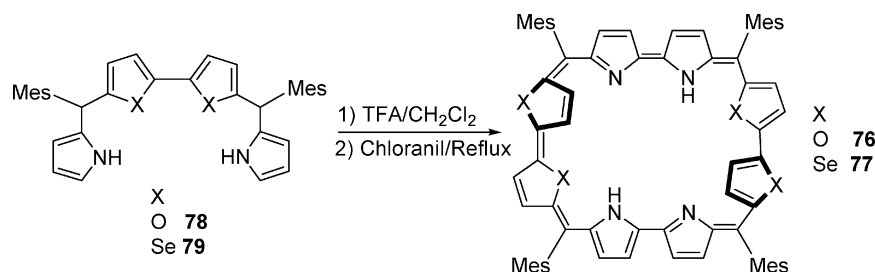
Confirmation of the flat structure for **75a** was obtained from a single-crystal X-ray analysis. The structure confirms (Figure 8) the inversion of one thiophene ring in each of the bithiophene units. The dihedral angle for the inverted thiophene with respect to the mean plane defined by the four *meso* carbon atoms is  $4.67^\circ$ . The planarity of the macrocycle excluding the *meso* mesityl ring is obvious from the side view (Figure 8). There are four intramolecular hydrogen-bonding interactions inside the cavity: two involving C-H $\cdots$ N ( $3.378$  Å,  $115.88(0)^\circ$ ) and two involving N-H $\cdots$ S ( $3.099$  Å,  $131.43(0)^\circ$ ), and these interactions are responsible for the complete flat structure observed for **75a**. In **75b**, the hydrogen atoms are found on the pyrrole nitrogens which are adjacent to the inverted thiophene ring. To avoid the repulsion between the N-H proton and

the inverted ring C-H protons, the heterocyclic ring is tilted out of the porphyrin plane making the ring non-planar as observed in the X-ray structure (Figure 8). The furan and selenophene containing octaphyrins **76** and **77** were also synthesized by an oxidative coupling reaction involving modified tetrapyranes **78** and **79** (Scheme 21).<sup>29</sup>

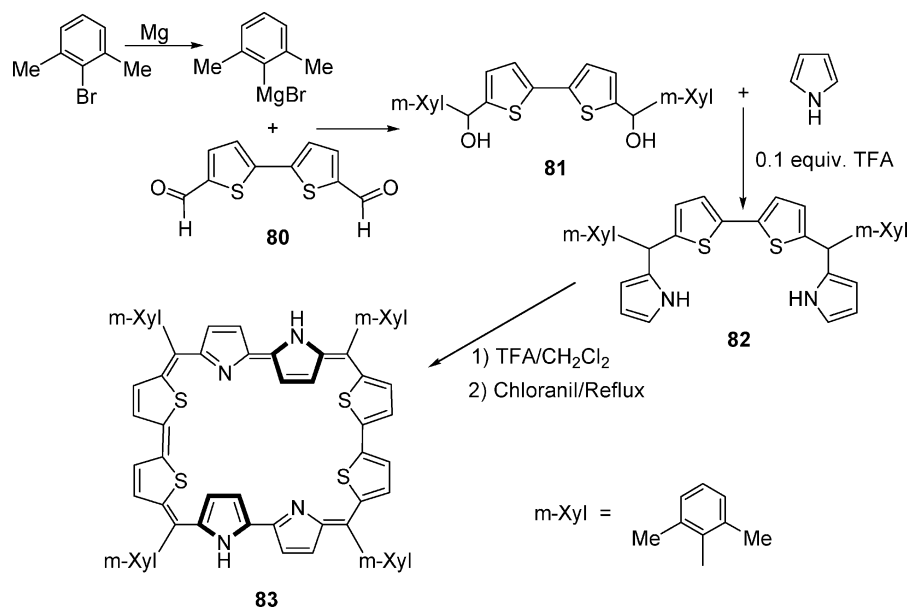
The site of ring inversion was found to be dependent on the nature of the *meso* substituent. A change of the *meso* mesityl substituent to *m*-Xylyl substituent resulted in the inversion of pyrrole rings rather than thiophene rings. The required precursor **82** was synthesized in a modified way from bithiophene dialdehyde **80**. **80** was further reduced to corresponding diol **81**, which on reaction with pyrrole gave tetrapyrane **82**. Subjecting **82** for an oxidative coupling reaction gave the desired octaphyrin, **83**, in 7% yield (Scheme 22).

Very recently Sessler and co-workers<sup>30</sup> reported the successful synthesis of a series of cyclooctapyrroles **84** bearing various  $\beta$  substituents without any *meso* carbons (Scheme 23). They have utilized a modified oxidative coupling procedure that involved the use of Fe(III) as the oxidant and novel biphasic reaction conditions to get octaphyrins **84** greater than 70%. This is one of the most effective examples of a one pot reaction in porphyrin chemistry, and one that highlights the utility of oxidative coupling strategies. These systems display features that are consistent with Huckel type  $4n + 2$  aromaticity. Recently, Latos-Grazynski and co-workers<sup>31</sup> reported a one pot synthesis of tetrathia octaphyrin **86** from Rothmund reaction of thiophene diol **87** and pyrrole followed by oxidation (Scheme 24). The  $^1\text{H}$  NMR spectroscopic studies

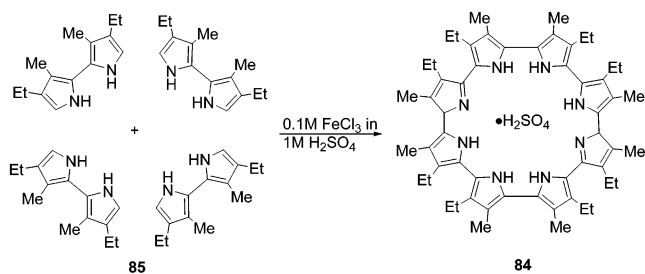
Scheme 21



Scheme 22



Scheme 23



and energy optimization methods provide support for a twisted conformation for **86**. It was found that the **86** exists in both reduced form (38  $\pi$ -electron) and oxidized form (36  $\pi$ -electron), which can be interconverted by exposure to appropriate conditions.

**4.1. Anion Binding Studies.** The first clue that the cyclooctapyrroles can act as anion receptors was obtained from the solid-state structure of sulfate bound<sup>30</sup> cyclooctapyrrole **84**. A single crystal X-ray analysis reveals that the diprotonated macrocycle is essentially planar with a sulfate ion centrally bound in the cavity of **84**. Eight N–H $\cdots$ O hydrogen bonding interactions in the solid state hold the anion and the N–H $\cdots$ O distances range from 1.91 to 2.49 Å. All four sulfate oxygens are involved in hydrogen bonding with the eight pyrrolic NH sites (Figure 9).

The protonated modified *meso* aryl octaphyrins **75**–**77** also bind TFA anion in 1:2 ratio.<sup>29</sup> Specifically, the TFA

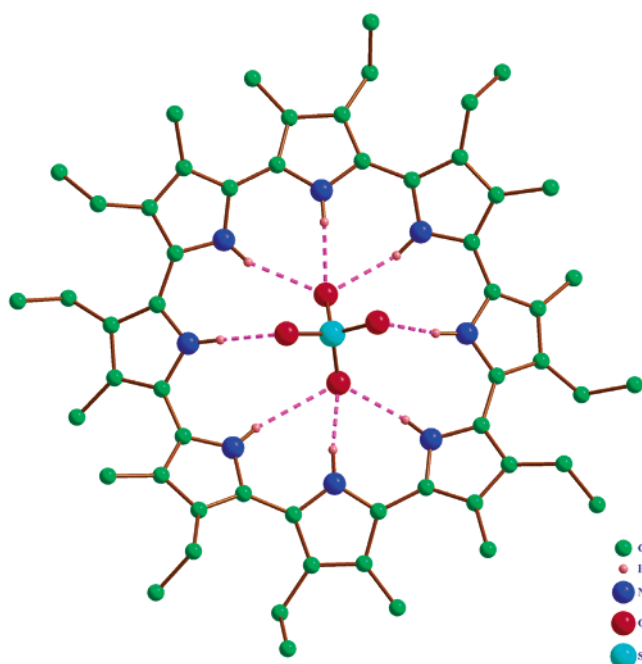


FIGURE 9. X-ray structure of sulfate adduct of **84**. [Reproduced from ref 30 with permission].

anion complex of **77**·(TFA)<sub>2</sub> displays a fairly flat structure similar to that of tetrathia octaphyrin **75** (Figure 10). The planarity of the macrocycle is slightly disrupted, probably

Scheme 24

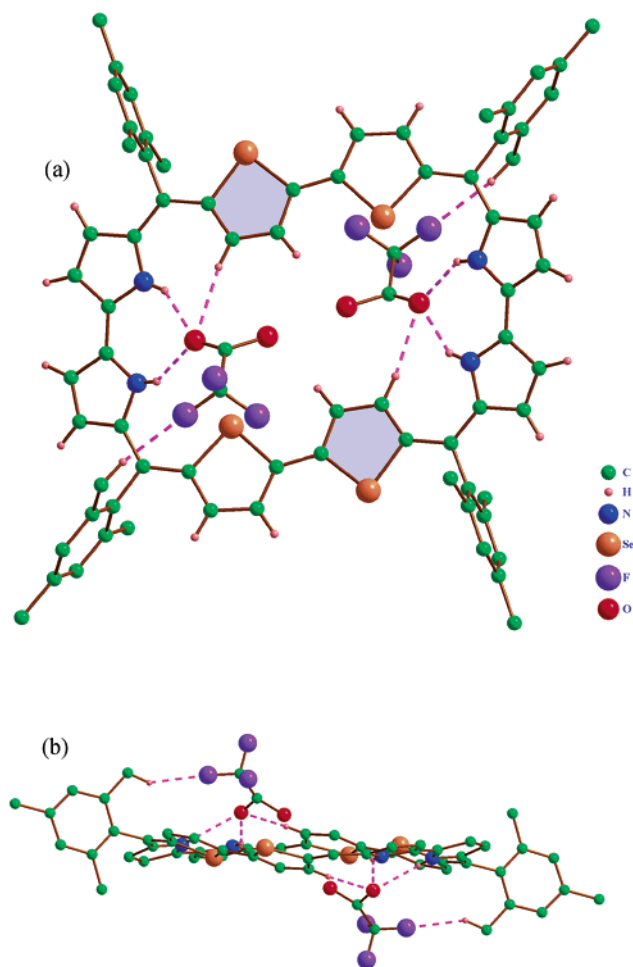
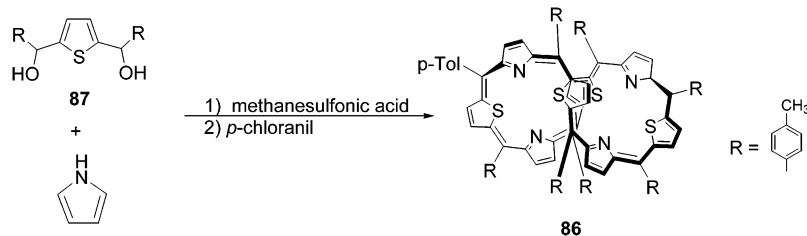


FIGURE 10. X-ray structure of  $77 \cdot (\text{TFA})_2$ . (a) top view (b) side view. The dotted lines show hydrogen bonding interactions.

owing to binding of the anions. Four hydrogen bonding interactions are found to be responsible for the binding of each TFA ion. They are (i)  $\text{N2-H}\cdots\text{O1}$  (2.232 Å, 143.67°), (ii)  $\text{N2-H}\cdots\text{O1}$  (2.139 Å, 146.64°), (iii)  $\text{C11-H}\cdots\text{O1}$  (2.444 Å, 171.04°) and (iv)  $\text{C34-H}\cdots\text{F2}$  (2.323 Å, 146.22°). Of the above four interactions, the first two are typical electrostatic interactions. The other two interactions are induced probably due to the geometric features of the interaction between the anion and the host macrocycle. The  $\beta$ -CH of the inverted selenophene ring forms a strong hydrogen bond with the -OH group in TFA. The proximity for the interaction is clearly evident from the near-linear bond angle, which is thought to be one of the key causes for the existence of this hydrogen bond. Such an interaction

is most consistent with a complete inversion of the selenophene ring.

## 5. Concluding Remarks

Improvements over the last five to six years in the chemistry of acyclic precursors required for accessing expanded porphyrins is one of the primary reasons for the rapid advancement of expanded porphyrin chemistry. Syntheses of an array of expanded porphyrins with larger  $\pi$ -electron delocalization pathways is being achieved and their diverse structural features well understood. Efforts are underway for their applications as anion receptors<sup>1a,5</sup> and as sensitizers for the PDT.<sup>1b,32</sup> It is satisfying to note that a variety of expanded porphyrins are awaiting different phases of trials for approval as radiation sensitizing drugs.<sup>32</sup> As for aromaticity, several examples discussed in this account clearly suggests that it is possible to design planar heteroatom annulenes containing up to 34  $\pi$  electrons that obey the  $4n + 2$  Huckel rule exhibiting aromatic character.

Material chemistry<sup>1c</sup> is another area, where expanded porphyrins could find application. Porphyrins and expanded porphyrins are among the most effective optical emitters in the visible region known to date, and their greater thermal stability, extended  $\pi$ -conjugation, ease of chemical modifications both in periphery, and core to tune the optical and electronic properties make them attractive targets as nonlinear optical materials for optoelectronics. There is considerable research activity in this area, and the recent observation of a large third-order optical susceptibility of self-assembled porphyrin oligomer<sup>33</sup> ( $\chi^3$  is on the order of  $1.0 \times 10^{-9}$  esu) and the conjugated porphyrin tapes<sup>34</sup> with electronic absorption into infrared region augurs well for their use as photoelectronic materials. Interestingly, the third-order optical susceptibility measured by Z scan method on one of the core-modified oxybenzporphyrin<sup>35</sup> from our laboratory shows a value of  $4.8 \times 10^{-13}$  SI units, and it is our hope that the availability of easy and efficient methodologies will stimulate more research in this area and the specific photonic applications using expanded porphyrins will become a reality soon.

*The work summarized in this account was supported by grants to T.K.C. from the Department of Science and Technology, New Delhi, India, and the Council of Scientific and Industrial Research, New Delhi, India. A large number of talented co-workers have significantly contributed to the work reported in this review. Our sincere thanks go to A. Srinivasan, B. Sridevi, S.J. Narayanan, Simi K. Pushpan, V.G. Anand, J. Sankar, Harapriya Rath, and V.*

Prabhuraja. We thank Prof. G. R. Desiraju for encouraging us to write this article.

## References

- (1) (a) Sessler, J. L.; Gebauer, A.; Weghorn, S. J. Expanded Porphyrins. In *Porphyrim Handbook*; Kadish, K. M., Smith, K. M., Guillard, R., Eds.; Academic Press: San Diego, 1999; Vol. II, Chapter 9. (b) Pandey, R. K.; Zheng, G. Porphyrins as Photosensitizers in Photodynamic Therapy. In *Porphyrim Handbook*; Kadish, K. M., Smith, K. M., Guillard, R., Eds.; Academic Press: San Diego, 1999; Vol. VI, Chapter 43. (c) Chou, J. H.; Nalwa, H. S.; Kosal, M. E.; Rakow, N. A.; Suslick, K. S. Applications of Porphyrins and Metalloporphyrins to Materials Chemistry. In *Porphyrim Handbook*; Kadish, K. M., Smith, K. M., Guillard, R., Eds.; Academic Press: San Diego, 1999; Vol. VI, Chapter 41. (d) Latos-Grazynski, L. Core-Modified Heteroanalogues of Porphyrins and Metalloporphyrins. In *Porphyrim Handbook*; Kadish, K. M., Smith, K. M., Guillard, R., Eds.; Academic Press: San Diego, 1999; Vol. II, Chapter 14.
- (2) (a) Lash, T. D. Porphyrin Synthesis by the "3+1" Approach: New Applications for an Old Methodology. *Chem. Eur. J.* **1996**, *2*, 1197–1200. (b) Srinivasan, A.; Mahajan, S.; Kumar, M. K.; Pushpan, S. K.; Chandrashekar, T. K. Synthesis of *Meso*-substituted core-modified expanded porphyrins: Effect of acid catalysts on the cyclization. *Tetrahedron Lett.* **1998**, *39*, 1961–1964. (c) Pushpan, S. K.; Anand, V. G.; Venkatraman, S.; Srinivasan, A.; Gupta, A. K.; Chandrashekar, T. K. Characterization of a new *meso*-Aryl isomer of Rubyrin:[26] Hexaphyrin (1.1.1.0.1.0) with an inverted heterocyclic ring. *Tetrahedron Lett.* **2001**, *42*, 3391–3394.
- (3) (a) Narayanan, S. J.; Srinivasan, A.; Sridevi, B.; Chandrashekar, T. K.; Senge, M. O.; Sugiura, K.-I.; Sakata, Y. Structural Diversity in Rubyrins: X-ray Structural Characterization of Planar and Inverted Rubyrins. *Eur. J. Org. Chem.* **2000**, 2357–2360. (b) Srinivasan, A.; Anand, V. G.; Narayanan, S. J.; Pushpan, S. K.; Kumar, M. R.; Chandrashekar, T. K.; Sugiura, K.-I.; Sakata, Y. Structural Characterisation of *meso* aryl Sapphyrins. *J. Org. Chem.* **1999**, *64*, 8693.
- (4) (a) Pushpan, S. K.; Srinivasan, A.; Anand, V. G.; Venkatraman, S.; Chandrashekar, T. K.; Joshi, B. S.; Roy, R.; Furuta, H. N-Confused Expanded Porphyrin: First Example of a Modified Sapphyrin with an Inverted N-Confused Pyrrole Ring. *J. Am. Chem. Soc.* **2001**, *123*, 5138–5139.
- (5) Sessler, J. L.; Davis, J. M. Sapphyrins: Versatile Anion Binding Agents. *Acc. Chem. Res.* **2001**, *34*, 989–997.
- (6) Sessler, J. L.; Morishima, T.; Lynch, V. Rubyrin: A New Hexapyrrolic Expanded Porphyrin. *Angew. Chem., Int. Ed. Engl.* **1991**, *30*, 997–980.
- (7) Vogel, E.; Pohl, M.; Herrmann, A.; Wiss, T.; Konig, C.; Lex, J.; Gross, M.; Gisselbrecht, J. P. Porphyrinoid Macrocycles Based on Thiophene-The Octaethyltetrathia-porphyrin Dication. *Angew. Chem., Int. Ed. Engl.* **1996**, *35*, 1529–1524.
- (8) Hu, Z.; Atwood, J. L.; Cava, M. P. A Simple Route to Sulfur Bridged Annulenes. *J. Org. Chem.* **1994**, *59*, 8071–8075.
- (9) Johnson, M. R.; Miller, D. C.; Bush, K.; Becker, J. J.; Ibers, J. A. Synthesis and Characterization of a New 26  $\pi$ -Aromatic Thiophene-Containing Macrocyclic Ligand. *J. Org. Chem.* **1992**, *57*, 4414–4417.
- (10) Srinivasan, A.; Reddy, V. R. M.; Narayanan, S. J.; Sridevi, B.; Pushpan, S. K.; Kumar, M. R.; Chandrashekar, T. K. Tetrathia- and Tetraoxarubyrins: Aromatic, Core-Modified Expanded Porphyrins. *Angew. Chem., Int. Ed. Engl.* **1997**, *36*, 2598–2601.
- (11) Srinivasan, A.; Pushpan, S. K.; Kumar, M. R.; Chandrashekar, T. K.; Roy, R. Novel Heteroatom Containing Rubyrins. *Tetrahedron* **1999**, *55*, 6671–6680.
- (12) Paolesse, R.; Jaquinod, L.; Nurco, D. J.; Mini, S.; Sagone, F.; Boschi, T.; Smith, K. M. 5,10,15-Triphenylcorrole: a product from a modified Rothemund reaction. *Chem. Commun.* **1999**, 1307–1308.
- (13) Narayanan, S. J.; Sridevi, B.; Chandrashekar, T. K.; Vij, A.; Roy, R. Sapphyrin Supramolecules through C-H $\cdots$ S and C-H $\cdots$ Se Hydrogen Bonds: First Structural Characterization of *meso*-Arylsapphyrins Bearing Heteroatoms. *Angew. Chem., Int. Ed. Engl.* **1998**, *37*, 3394–3397.
- (14) Narayanan, S. J.; Sridevi, B.; Chandrashekar, T. K.; Vij, A.; Roy, R. Novel Core-Modified Expanded Porphyrins with *meso*-Aryl Substituents: Synthesis, Spectral and Structural Characterization. *J. Am. Chem. Soc.* **1999**, *121*, 9053–9068.
- (15) (a) Narayanan, S. J.; Sridevi, B.; Chandrashekar, T. K. Core-Modified Smaragdyrins: First Examples of Stable *Meso*-Substituted Expanded Corrole. *Org. Lett.* **1999**, *1*, 587–590. (b) Sridevi, B.; Narayanan, S. J.; Chandrashekar, T. K.; Englisch, U.; Senge, K. R. Core-Modified *meso*-Aryl Corrole: First Example of Cu<sup>II</sup>, Ni<sup>II</sup>, Co<sup>II</sup> and Rh<sup>I</sup> complexes. *Chem. Eur. J.* **2000**, *6*, 2554–2563.
- (16) Sessler, J. L.; Seidel, D.; Bucher, C.; Lynch, V. [26] Hexaphyrin (1.1.1.1.0.0): an all-aza isomer of rubyrin with an inverted pyrrole subunit. *Chem. Commun.* **2000**, 1473–1474.
- (17) Narayanan, S. J.; Venkatraman, S.; Anand, V. G.; Chandrashekar, T. K. *Meso*-mesityl dithia- and diselenarubyrins: existence of planar and inverted forms in solution. *J. Porphyrins Phthalocyanines* **2002**, *6*, 403–409.
- (18) Narayanan, S. J.; Sridevi, B.; Chandrashekar, T. K.; Englisch, U.; Senge, K. R. Interaction of Rh(I) with *meso*-Arylsapphyrins and Rubyrins: First Structural Characterization of Bimetallic Heterorubyrin Complex. *Inorg. Chem.* **2001**, *40*, 1637–1645.
- (19) Srinivasan, A.; Anand, V. G.; Narayanan, S. J.; Pushpan, S. K.; Chandrashekar, T. K.; Sugiura, K.-I.; Sakata, Y. Core-modified *meso*-aryl sapphyrins and rubyrins: structural and anion receptor properties. *J. Chem. Soc., Perkin Trans. 2* **2000**, 1788–1793.
- (20) Sessler, J. L.; Seidel, D.; Lynch, V. Synthesis of [28] Heptaphyrin (1.0.0.1.0.0.0) and [32] Octaphyrin (1.0.0.0.1.0.0.0) via a Directed Oxidative Ring Closure: The First Expanded Porphyrins Containing a Quaterpyrrole Subunit. *J. Am. Chem. Soc.* **1999**, *121*, 11257–11258.
- (21) Anand, V. G.; Pushpan, S. K.; Srinivasan, A.; Narayanan, S. J.; Sridevi, B.; Chandrashekar, T. K.; Roy, R.; Joshi, B. S. *Meso* Aryl Heptaphyrins: The First 30  $\pi$  Aromatic Expanded Porphyrins with an Inverted Structure. *Org. Lett.* **2000**, *2*, 3829–3832.
- (22) Anand, V. G.; Pushpan, S. K.; Venkatraman, S.; Narayanan, S. J.; Dey, A.; Chandrashekar, T. K.; Roy, R.; Joshi, B. S.; Deepa, S.; Sastry, G. N. 30  $\pi$  Aromatic *Meso*-Substituted Heptaphyrin Isomers: Syntheses, Characterization and Spectroscopic Studies. *J. Org. Chem.* **2002**, *67*, 6309–6319.
- (23) Bucher, C.; Seidel, D.; Lynch, V.; Sessler, J. L. [30] Heptaphyrin (1.1.1.1.1.0.0): an aromatic expanded porphyrin with a 'figure eight' like structure. *Chem. Commun.* **2002**, 328–329.
- (24) Vogel, E.; Broring, M.; Fink, J.; Rosen, D.; Schmickler, H.; Lex, J.; Chan, K. W. K.; Wu, Y.-D.; Plattner, D. A.; Nendel, M.; Houk, K. N. From Porphyrin Isomers to Octapyrrolic "Figure Eight" Macrocycles. *Angew. Chem., Int. Ed. Engl.* **1995**, *34*, 2511–2514.
- (25) (a) Broring, M.; Jendry, J.; Zander, L.; Schmickler, H.; Lex, J.; Wu, Y.-D.; Nendel, M.; Chen, J.; Plattner, D. A.; Houk, K. N.; Vogle, E. Octaphyrin-(1.0.1.0.1.0.1.0). *Angew. Chem., Int. Ed. Engl.* **1995**, *34*, 2515–2517. (b) Wytko, J.; Michels, M.; Zander, L.; Lex, J.; Schmickler, H.; Vogel, E. Competitive Formation of Helical Cycloocta- and Cyclododecapyrroles. *J. Org. Chem.* **2000**, *65*, 8709–8714.
- (26) Setsune, J.-I.; Katakami, Y.; Lizuna, N. [48] Dodecaphyrin (1.0.1.0.1.0.1.0.1.0.1.0) and [64] Hexadecaphyrin (1.0.1.0.1.0.1.0.1.0.1.0.1.0.1.0.1.0): The Largest Cyclopolypyrroles. *J. Am. Chem. Soc.* **1999**, *121*, 8957–8958.
- (27) Shin, J.-Y.; Furuta, H.; Yoza, K.; Igarashi, S.; Osuka, A. *meso*-Aryl-substituted Expanded Porphyrins. *J. Am. Chem. Soc.* **2001**, *123*, 7190–7191.
- (28) Anand, V. G.; Pushpan, S. K.; Venkatraman, S.; Dey, A.; Chandrashekar, T. K.; Joshi, B. S.; Roy, R.; Teng, W.; Senge, K. R. 34  $\pi$  Octaphyrin: First Structural Characterization of a Planar, Aromatic [1.0.1.0.1.0.1.0] Octaphyrin with Inverted Heterocyclic Rings. *J. Am. Chem. Soc.* **2001**, *123*, 8620–8621.
- (29) Anand, V. G.; Venkatraman, S.; Rath, H.; Chandrashekar, T. K.; Teng, W.; Senge, K. R. *Meso* substituted aromatic 34  $\pi$  core-modified octaphyrins: Syntheses, Characterization and anion binding properties. *Chem. Eur. J.* **2003**, *9*, 2282–2290.
- (30) Seidel, D.; Lynch, V.; Sessler, J. L. Cyclo[8]pyrrole: A simple-to-make Expanded Porphyrin with no *Meso* Bridges. *Angew. Chem., Int. Ed. Engl.* **2002**, *41*, 1422–1425.
- (31) Sprutta, N.; Latos-Grazynski, L. Figure-Eight Tetrathiaoctaphyrin and Dihydrotetrathiaoctaphyrin. *Chem. Eur. J.* **2001**, *7*, 5099–5112.
- (32) Sharman, W. M.; Allen, C. M.; van Lier, J. E. Photodynamic therapeutics: basic principles and clinical application. *DDT.* **1999**, *4*, 507–517.
- (33) (a) Ogawa, K.; Zhang, T.; Yoshihara, K.; Kobuke, Y. Large Third-Order Optical Nonlinearity of Self-Assembled Porphyrin Oligomers. *J. Am. Chem. Soc.* **2002**, *124*, 22–23.
- (34) Tsuda, A.; Osuka, A. Fully Conjugated Porphyrin Tapes with Electronic Absorption Bands that reach into Infrared. *Science* **2001**, *293*, 79–82.
- (35) Venkatraman, S.; Anand, V. G.; Pushpan, S. K.; Sankar, J.; Chandrashekar, T. K. Core-Modified oxybenzporphyrins: new aromatic ligand for metal-carbon bond activation. *Chem. Commun.* **2002**, 462–463.

AR020284N